

Recombination light emission by molybdenum bombarded by slow electrons

P. G. Borzyak, I. I. Geguzin, V. N. Datsyuk, I. A. Konovalov, Yu. A. Kulyupin, and K. N. Pilipchak

Institute of Physics of the Academy of Sciences of the Ukrainian SSR
(Submitted 15 August 1980)
Zh. Eksp. Teor. Fiz. **80**, 1514–1523 (April 1981)

The spectra of light emitted by molybdenum bombarded by slow electrons are measured. A model is proposed which can be used to calculate the spectrum of the light emitted by a metal on excitation of nonequilibrium carriers in it. The spectra expected on the basis of a self-consistent calculation of the band structure of molybdenum by the Korrinya-Kohn-Rostoker technique are presented. It is shown that the emission spectrum is mainly determined by direct interband recombination of electrons with holes located below the Fermi level and generated by the bombarding electrons. The radiation yield is estimated and found to be in agreement with measured value.

PACS numbers: 79.20.Kz

1. INTRODUCTION

Up until recently, recombination emission of light (well known in dielectrics and semiconductors) has been considered to be of negligibly low probability in metals.¹ However, it has been observed that on interaction of metals with photons,² x-ray beams,³ slow electrons,^{4,5} ions,⁶ atoms, and molecules emission occurs in the visible region of the spectrum; it has been suggested that the observed light emission is at least partially connected with radiative recombination of the nonequilibrium carriers produced in this case in the metal.^{2,6-9}

Our work is devoted to an experimental investigation of the light emission on bombardment of molybdenum by slow electrons, and to the clarification of the possibility of attributing its characteristics to interband transitions. We chose to study molybdenum firstly, because methods are known for obtaining an atomically pure metal surface; secondly, because calculations of the electronic structure of molybdenum are available and can explain the results of the optical, photoelectron, and x-ray studies. It is also known that the plasma-oscillation frequency in molybdenum is about 10 eV, i. e., the corresponding singularities of the spectra of molybdenum are located in the vacuum ultraviolet. Slow electrons, as a source of excitation of nonequilibrium carriers, are the most suitable because in this case no doubts arise concerning the contribution of transition radiation or bremsstrahlung. Furthermore, we may change the parameters of a beam of slow electrons relatively easily within broad limits. In this case, the maximum in the density of nonequilibrium carriers is reached at a distance from the surface which is equal to several lattice constants; thus we may neglect the possible change in the electronic structure of molybdenum at its surface.

2. CALCULATION OF THE LIGHT EMISSION SPECTRUM

2.1 Initial models

The one-electron band model is the basis of the theoretical consideration of the light emission by a bulk

metal bombarded by slow electrons. The basic assumption is that, as a consequence of bombardment by slow electrons, a steady-state density of nonequilibrium electrons and holes is maintained in the metal; these may emit light on relaxing to the ground state. In particular, a hole generated in the valence band is filled by a higher-lying electron. This (along with other processes) should also lead to light emission. This notion concerning the nature of light emission from metals bombarded by slow electrons was advanced earlier⁵ and is analyzed numerically in this paper for the first time.

The ground state of the electron system of a crystal is described by a set of Bloch functions ψ_{jk} , to which correspond one-electron energies E_{jk} , where j is the band number and k is the wave vector in the given Brillouin zone. Let us consider the direct and indirect transition models separately.

In the dipole approximation, the probability of a direct interband transition between the initial state i and the final state f is proportional to the square of the modulus of the momentum-operator matrix element

$$\tilde{M}_{if}(\mathbf{k}) = \langle f\mathbf{k} | \mathbf{np} | i\mathbf{k} \rangle. \quad (1)$$

Such a transition is accompanied by emission of a photon with energy $\hbar\omega$:

$$E_i - E_f = +\hbar\omega. \quad (2)$$

In the direct transition model, the total contribution to the emission of light at frequency ω is determined by the integral over the Brillouin zone and the sum over all band pairs:

$$J_{\text{dir}}^+(\omega) \sim \omega \sum_i \sum_f \int d^3k |M_{if}(\mathbf{k})|^2 F_{i\mathbf{k}}(1 - F_{f\mathbf{k}}) \delta(E_{f\mathbf{k}} - E_{i\mathbf{k}} + \hbar\omega). \quad (3)$$

Here $F_{i\mathbf{k}}$ and $F_{f\mathbf{k}}$ are the distribution functions of the initial and the final states. In the approximation which assumes a constant momentum matrix element, we find that the emission spectrum in this model is connected with the joint density of states:

$$J_{\text{dir}}^+ = \frac{2}{(2\pi)^3} \sum_i \sum_f \int d^3k F_{i\mathbf{k}}(1 - F_{f\mathbf{k}}) \delta(E_{f\mathbf{k}} - E_{i\mathbf{k}} + \hbar\omega), \quad (4)$$

and the photon emission rate measured in experiment is

$$N_{\omega}(\omega) \sim \omega J_{\text{dir}}^{+}(\omega). \quad (5)$$

Within the framework of the indirect transition model, in analogy with Eq. (4) we may introduce a joint density-of-states function

$$J_{\text{indir}}^{+}(\omega) = \frac{4}{(2\pi)^6} \sum_j \sum_k \int d^3k_1 \int d^3k_2 F_{i k_1} (1 - F_{j k_2}) \delta(E_{j k_2} - E_{i k_1} + \hbar\omega) = \mathcal{N}_j^{*}(\omega) * \mathcal{N}_i(\omega + \hbar\omega), \quad (6)$$

where * indicates the convolution of the density of final states \mathcal{N}_j and the density of initial states \mathcal{N}_i :

$$\mathcal{N}(E) = \frac{2}{(2\pi)^3} \sum_j \int d^3k \delta(E - E_{j k}). \quad (7)$$

One of the least studied questions involves the distribution functions of the nonequilibrium excitations in the metal ($F_{i k}$ and $F_{j k}$). In this work we assume that there is some nonequilibrium distribution of electrons and holes which is characterized by zero temperature and by the fact that:

1) the level population by electrons at $E < E_F$ is equal to $1 - C_1$, where $C_1 \ll 1$ does not depend on the energy and on number of the band; then the probability of transition of an electron to a lower-lying hole is proportional to $C_1(1 - C_1) \approx C_1$ to within terms of second-order;

2) the level population by electrons at $E > E_F$ is $C_2 = \text{const}$; then the probability of transition of an electron to a lower-lying hole is proportional to $C_2(1 - C_2) \approx C_2$, since $C_2 \ll 1$.

In such a model, we may neglect recombination transitions of electrons with $E > E_F$ to holes with $E < E_F$, since the probability for such transitions is proportional to $C_1 C_2$. We may assume that C_1 and C_2 are independent of energy only as a zero-order approximation. Some justification for such a choice may come from the success of this simple model in explaining the ionoluminescence spectra of metals.⁶

Within the assumptions described above, we calculated the joint densities of states $J_{\text{dir}}^{+}(\omega)$ and $J_{\text{indir}}^{+}(\omega)$, for which we need to know the band structure of Mo.

2.2 Calculation of the band structure and emission spectra of Mo

Although the results of band-structure calculations for Mo are described in the literature, we could not use them to calculate the emission spectrum, owing to the limited information contained in the papers. Therefore, in this work we carried out a self-consistent calculation of the band structure of Mo by the Korringa-Kohn-Rostoker method, the details of which are given in Ref. 10. Self consistency was achieved for a poten-

TABLE I. Characteristic interband separations in molybdenum.

Energy gap	Our work	[13]
$s-d$ splitting, $\Gamma_{25} - \Gamma_1$	0.402	0.408
$s-d$ splitting, $\Gamma_{12} - \Gamma_1$	0.606	0.596
Width of d band, $H_{32} - H_{12}$	0.749	0.888

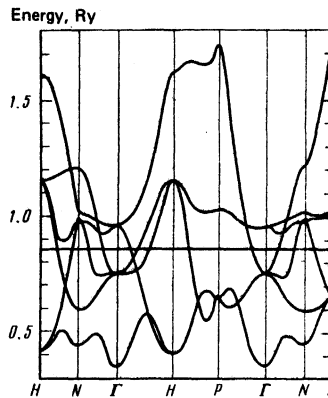


FIG. 1. Dispersion law $E_j(\mathbf{k})$ for electrons in molybdenum along several symmetry directions in \mathbf{k} space.

tial model characterized by specifying the lattice parameter, the "muffin-tin" sphere radius, and the parameter α in the exchange-correlation part of the potential. For the latter, we took a value determined from the condition that the total energy $X\alpha$ of an isolated atom equal the Hartree-Fock energy.¹¹ The Coulomb part of the potential was calculated with formulas of Ref. 12.

The calculation of the band structure for the self-consistent potential was carried out at 55 points of the irreducible part of the Brillouin zone, which formed a cubic mesh with step $2\pi/a$ in \mathbf{k} space (1/8, 1/8, 1/8). On Fig. 1 we show the dispersion law for the lowest six bands along several symmetry directions in \mathbf{k} space. Our results agree (Table I), with respect to the $s-d$ splitting, with the results of a non-self-consistent calculation¹³ in which the value $\alpha = 1$ was taken for the exchange parameter. They lead, however, to a d band that is broader by 0.8 eV. This difference is due to the use of $\alpha = \alpha_{HF}$ and the self-consistent calculation of the potential, which is a more consistent embodiment of the idea of a band calculation "from first principles."

In order to find the energy distribution of the density of the electronic states $\mathcal{N}(E)$ we used a mathematical interpolation scheme, the details of which have been described previously.¹⁴ The energies are calculated at 91 520 points of the irreducible part of the Brillouin zone, corresponding to 4 194 304 points of the entire zone. The width of the histogram rectangle is 0.01 Ry, which gives an approximate relative error of 1.5% in

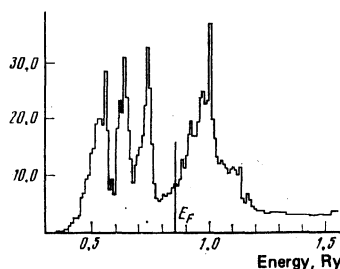


FIG. 2. Energy distribution of the density of electronic states $\mathcal{N}(E)$, electrons/atom · Ry, of the six lowest bands in Mo; E_F is the Fermi level.

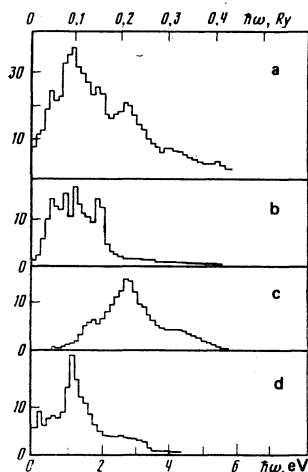


FIG. 3. Transition energy distribution of the joint density of states $J_{\text{dir}}^+(\omega)$, electrons/atom \cdot Ry. (a), and the contribution to the total histogram for the different band pairs: (b) 2 \rightarrow 1; (c) 3 \rightarrow 1; (d) 3 \rightarrow 2.

the ordinate of the histogram (Fig. 2). The Fermi level is determined by the occupation of a unit cell by five electrons, and is equal to 0.859 Ry.

With the same statistical accuracy as for $\mathcal{N}(E)$, the transition energy distribution was calculated for the joint densities of states $J_{\text{dir}}^+(\omega)$ and $J_{\text{indir}}^+(\omega)$ that determine the shape of the optical emission spectrum. On Fig. 3 we show how the contributions of transitions between different bands produce the shape of $J_{\text{dir}}^+(\omega)$, considering a model in which both the initial and the final states are located below the Fermi level ($C_2 = 0$). It is interesting to note that in the energy range from 2 to 4 eV, the primary contribution to the emission spectrum comes from the single pair of bands 3 \rightarrow 1, while the transitions 2 \rightarrow 1 and 3 \rightarrow 2 are in the energy region below 2 eV. The emission spectrum $N_\omega(\omega)$ corresponding to this $J_{\text{dir}}^+(\omega)$ is given on Fig. 4(a). The results of the calculation of $N_\omega(\omega)$ on the basis of $J_{\text{indir}}^+(\omega)$, performed under the same assumptions, are given on Fig. 4(b), while on Fig. 4(c), we give the light emission spectrum calculated in the direct-transition model for the case when both the initial and the final state are located above the Fermi level ($C_1 = 0$). In this case account is taken of electrons that occupy bands up to the sixth inclusively, including those located above the vacuum levels. The seventh band only very weakly overlaps the top of the sixth band,¹³ so that if a restricted spectral interval of interband transitions is considered we do not introduce errors by taking into account only the six lowest bands.

The results presented are evidence of the rather high sensitivity of the theoretical spectra to the details of the band structure. Thus, neglect of contributions from transitions with participation of a single band substantially changes the shape of the emission spectrum (Fig. 3), and use of the non-self-consistent calculation (as in Ref. 13) leads to a spectrum shift that can be estimated at 0.4 eV, recognizing that the Fermi level in Mo passes approximately through the center of the d band, a very important factor in the optical wavelength range.

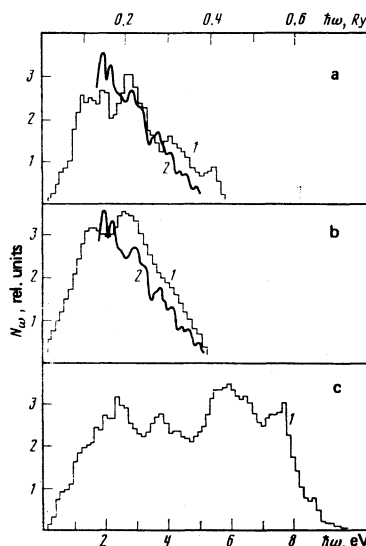


FIG. 4. The calculated light emission spectra of molybdenum in the direct transition model [(a), (c)] and the indirect transition model (b) (curves 1); the measured light emission spectrum of Mo (curves 2).

3. EXPERIMENTAL TECHNIQUE AND RESULTS

In the experiments, a beam of electrons with energy 200 eV was incident normally on the surface parallel to the (110) face of molybdenum. The emission could be recorded at various observation angles ranging from 15° to 85° (the observation angle is reckoned from the normal to the surface of the sample). The angle of incidence of the electrons on the surface was not varied.

The bombarded molybdenum target was a thin plate of thickness 300 μ . The technology for obtaining such samples from monocrystalline ingots of molybdenum (purified by crucibleless zone melting) is well known.¹⁵ According to the certified specifications, the primary impurities in the initial material were oxygen and carbon, the concentration of which was $(2 \pm 0.6) \cdot 10^{-6}$ and $(3 \pm 0.9) \cdot 10^{-6}$ wt.%, respectively. The ratio of the resistance at room temperature and at liquid helium temperature, which characterizes the chemical purity and the structural perfection of the initial crystals, was equal to $5 \cdot 10^4$. The target was decarbonized according to the technique of Refs. 16 and 17, which results in complete removal of the carbon from the crystal surface. Subsequent outgassing of the target was carried out by pulsed heating (the "flash" method) at a temperature of 2100°K. Chemisorbed oxygen, which is the gas most strongly bound to the surface, is completely desorbed at this temperature.¹⁸ After such flashing, the crystal surface became atomically pure.

The measurements were performed in an all-metal vacuum chamber at a pressure $p \leq 2 \cdot 10^{-9}$ Torr. A beam of slow electrons was generated using a four-electrode electron gun, which made it possible to obtain a monoenergetic beam of electrons with energies from 25 to 800 eV and a current density at the target of 1 mA/cm².

The optical emission induced when the target was bombarded by slow electrons was analyzed using a high-

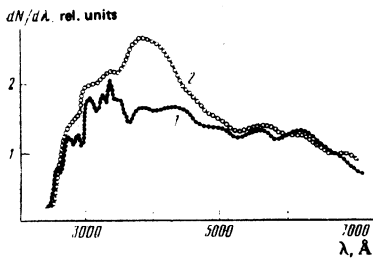


FIG. 5. Light emission spectrum of molybdenum before (2) and after (1) cleaning the surface of the crystal.

transmission monochromator. The light flux incident on the photomultiplier was recorded by a system operating in the photon-counting regime. The relative spectral sensitivity of the recording system was determined using standard tungsten, xenon, and mercury lamps.

The spectrum for the atomically pure surface was recorded within a time shorter than the time for deposition of a monolayer of the residual gases. The adsorption of residual gases on the clean molybdenum surface led to a slight ($\approx 9\%$) decrease in the integrated intensity of the emission. The intensity of the light emission increases with increasing current and energy of the exciting electrons.

Comparison of the emission spectra in the case of an atomically pure surface (Fig. 5, curve 1) and before the final purification of the crystal (curve 2) shows that the singularities of the emission spectrum before the final purification are much less pronounced. The most substantial difference is the presence of a broad band with a maximum in the 4000 Å region, which disappears after decarbonization of the crystal. All the details of the spectrum for the atomically pure surface are reproduced well. No substantial changes in the emission spectra as functions of observation angle were observed.

Measurement of the degree of polarization of the emission at different observation angles shows an increase in the degree of polarization, from 40% at an observation angle 15° to 96% for an angle 85° (Fig. 6). The preferred position of the electric vector of the light wave lies in this case in a plane containing the normal to the sample surface and the direction of observation. The degree of polarization of the emission is the same for different wavelengths. A change in the electron beam energy from 100 to 800 eV did not lead to a change

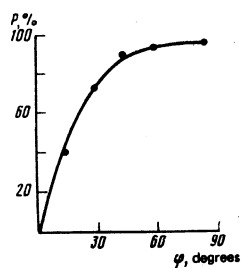


FIG. 6. Dependence of the degree of polarization of the emission on the observation angle.

in the degree of polarization of the emission at different observation angles and at different wavelengths.

4. DISCUSSION OF RESULTS

On Fig. 4 we compare the theoretical light-emission spectra with the experimental spectra transformed to a frequency scale. This comparison allows us to give preference to models in which both states lie below E_F [Figs. 4(a), (b)], since the primary qualitative characteristics of the spectrum—the decrease in intensity with increase in frequency and the existence of an upper limit of the spectrum—are reproduced. This may be due to the fact that the concentration C_2 of nonequilibrium electrons having an energy in a range several eV above E_F is appreciably less than the hole concentration C_1 .

This result could be expected also from general considerations. In fact, all phenomena on which various electron spectroscopy methods are based (characteristic-energy-loss spectroscopy, threshold-potential spectroscopy, Auger spectroscopy) ultimately result in excitation of holes in filled bands, just as in x-ray spectroscopy. Although the lifetime of holes in the deep-lying levels is short, we can expect the lifetime to be appreciably longer in a valence band below the Fermi level; furthermore, an Auger electron having an energy less than the work function of the metal generates fresh holes.

The direct-transition model [Fig. 4(a)] leads to a spectrum having a pronounced structure, while the indirect-transition transition model [Fig. 4(b)] leads to a markedly smoother spectrum. Analogous results are obtained on calculating the imaginary part of the permittivity $\epsilon_2(\omega)$ and the optical conductivity $\sigma(\omega) \sim \omega \epsilon_2(\omega)$, starting from the same band spectrum of Mo in the approximation assuming a constant transition matrix element. It turns out that the structure of the spectra in the direct-transition models [see Fig. 7(a)] has more pronounced hills and valleys than in the indirect-transition model [Fig. 7(b)], likewise in agreement with the published results.^{19,20}

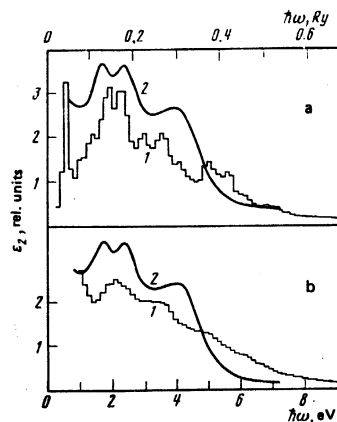


FIG. 7. Dependence of the imaginary part of the permittivity ϵ_2 on the frequency ω , calculated in the direct transition model (a) and in the indirect transition model (b) (curves 1); the spectrum of $\epsilon_2(\omega)$ measured in Ref. 22 (curves 2).

The singularities of the energy distribution of the joint densities of states $J_{\text{dir}}^+(\omega)$ and $J_{\text{indir}}^+(\omega)$ are of a different nature. In the indirect-transition model, these singularities can be directly associated with the structure of the energy distribution of the density of states $\mathcal{N}(E)$, something in the general case incorrect for the direct-transition model. Since the measured light-emission spectra have a distinct structure, and the positions of the maxima in the experimental and the theoretical spectra are correlated as a rule, we may obviously give preference to the direct-transition model. However, a detailed comparison of the spectra cannot be made until we take into account the population factors and the transition matrix elements in the integrand in Eq. (3). Clearly, the assumption that the momentum matrix element is constant may be taken only as a first approximation. Indeed, at several points in \mathbf{k} space (Γ, N, H) transitions between arbitrary pairs of the lower six bands are symmetry-forbidden (except for the transitions 1 \rightarrow 4 at N and 2 \rightarrow 6 at H). At general points of \mathbf{k} space, transitions are allowed between all pairs of bands. However, whatever the role of the matrix elements is, it is clear¹³ that they may not lead to new singularities in the spectral distributions of the joint densities of states.

The rate of spontaneous photon emission, calculated for a single selected interband transition with $\hbar\omega = 3.5$ eV, was equal to $6 \cdot 10^8$ s⁻¹. This allows us to estimate the order of magnitude of the average lifetime relative to radiative transitions at 10^{-8} s, and the contribution of radiative transitions to the width of the level at about 10^{-7} eV.

The change in the degree of polarization of the emission for different observation angles also makes it necessary to consider more thoroughly the emission model used, with the goal of obtaining information on the polarization characteristics of the emission. From general considerations it is obvious that radiative recombination of electrons and holes as a result of direct and indirect transitions, occurring within the bulk of the sample, can not lead to polarization of the emission, since summation of the individual photon-emission events occurs over the symmetric Brillouin zone. For emission at an angle relative to the surface, the light may in principle be partially polarized. The preferred direction of the electric vector of the light wave should correspond to that observed in the experiment (parallel to the plane of observation). However, it is difficult in this case to expect almost 90% polarization at an observation angle 45° .

We may hypothesize an important role for radiative recombination, with participation of the surface, occurring upon inelastic reflection of electrons from the surface of the crystal. Radiation caused by such surface recombination, according to Refs. 7 and 21, should be linearly polarized, and its angular distribution is determined by a factor of the form $\cos^2\theta$ (θ is the angle between the direction of observation and the surface). Thus, the polarization and angular characteristics of the emitted radiation are similar to those which would be possessed by a dipole located on the

surface, with the dipole axis normal to the surface. Since such a dipole does not radiate in a direction normal to the surface, at an observation angle 0° the emission should be completely unpolarized (determined only by the radiative recombination within the bulk of the sample); and at a grazing observation angle, it should be almost completely polarized. This trend in the change of the degree of polarization as a function of registration angle is indeed observed in experiment.

Yet, the experiment shows that the spectral distributions of the emission intensity are practically unchanged at different observation angles. Formally, this may be explained by the fact that in inelastic reflection of electrons from the potential barrier on the crystal surface, as in the case of radiative recombination within the bulk of the sample as a result of direct interband transitions, the expression for the spectral distribution of emission intensity proves to be proportional to $J_{\text{dir}}^+(\omega)$. The difficulty is connected with the possibility of using the $J_{\text{dir}}^+(\omega)$ obtained on the basis of a calculation of the wave functions of electrons within the bulk of the crystal, when radiative recombination with participation of the surface is considered. This question requires a special theoretical examination.

In order to be confident that the experimental results can be explained on the basis of ideas concerning recombination radiation of light in the metal, it is important to estimate the radiation yield and compare it with that measured experimentally. If we assume that the lifetime of nonequilibrium holes relative to an Auger transition is of the order of $10^{-14} - 10^{-15}$ s, while the lifetime relative to dipole radiation is of the order of 10^{-8} s, then the radiation yield should amount to $10^{-6} - 10^{-7}$ photons per Auger electron. At the same time it is known that the yield of Auger electrons is of the order of $10^3 - 10^4$ per incident electron. Consequently, we can expect a radiation yield $10^{-3} - 10^{-11}$ photons/electron, which is in reasonable agreement with the experimentally estimated yield 10^{-10} photons/electron for $E = 100$ eV.

¹L. N. Dobretsov and M. V. Gomoyunova, *Emissionnaya Elektronika* (Emission Electronics, Israel Program Sci.

Transl., Jerusalem, 1971), Nauka, Moscow, 1966, Ch. 7.

²A. Mooradian, *Phys. Rev. Lett.* **22**, 185 (1969).

³Th. Kokkinakis and K. Alexopoulos, *Phys. Rev. Lett.* **28**, 1632 (1972).

⁴O. M. Artamonov, *Zh. Tekh. Fiz.* **45**, 178 (1975). [*Sov. Phys. Tech. Phys.* **45**, 113 (1975)].

⁵P. G. Borzyak, A. N. Zaviopulo, Yu. A. Kulyupin, I. A. Konovalov, K. N. Pilipchak, and O. B. Shpenik, *Dopov. Akad. Nauk Ukr. SSR, Ser. A* **37**(8), 730 (1975).

⁶M. Zivitz and E. W. Thomas, *Phys. Rev.* **B13**, 2747 (1976).

⁷P. G. Borzyak, I. P. Zapesochnyi, I. A. Konovalov, V. A. Kritskii, Yu. A. Kulyupin, K. N. Pilipchak, S. S. Pop, and P. M. Tomchuk, *Izv. Akad. Nauk SSSR, Ser. Fiz.* **40**, 1621 (1976).

⁸P. G. Borzyak and Yu. A. Kulyupin, *Ukr. Fiz. Zh. (Russ. Ed.)* **24**, 204 (1979).

⁹O. M. Artamonov and S. N. Samarin, *Radiat. Eff.* **40**, 201 (1979).

- ¹⁰G. I. Al'ferovich, I. I. Geguzin, A. V. Nikol'skiĭ, V. G. Kochetov, and I. Ya. Nikiforov, *Izv. Akad. Nauk SSSR, Ser. Fiz.* **40**, 251 (1976).
- ¹¹K. Schwarz, *Theor. Chem. Acta* **34**, 225 (1974).
- ¹²V. V. Dyakin, R. F. Egorov, and V. P. Shirokovskii, *Fiz. Met. Metalloved.* **31**, 691 (1971).
- ¹³I. Petroff and C. R. Viswanathan, *Phys. Rev.* **B4**, 799 (1971).
- ¹⁴I. I. Geguzin, I. Ya. Nikiforov, and G. I. Al'ferovich, *Fiz. Tverd. Tela (Leningrad)* **15**, 931 (1973) [*Sov. Phys. Solid State* **15**, 646 (1973)].
- ¹⁵O. A. Panchenko, P. P. Lutsishin, and Yu. G. Ptushinskiĭ, *Zh. Teor. Eksp. Fiz.* **66**, 2191 (1974) [*Sov. Phys. JETP* **39**, 1079 (1974)].
- ¹⁶R. M. Stern, *Appl. Phys. Lett.* **5**, 218 (1964).
- ¹⁷B. M. Zykov, D. S. Ikopnikov, and V. K. Tskhakaya, *Fiz. Met. Metalloved.* **47**, 336 (1979).
- ¹⁸N. N. Vas'ko and Yu. G. Ptushinskiĭ, *Ukr. Fiz. Zh.* **13**, 1733 (1968).
- ¹⁹J. Yamashita, Y. Kubo, and S. Wakoh, *J. Phys. Soc. Jpn.* **42**, 1906 (1977).
- ²⁰D. D. Koelling, F. M. Mueller, and B. W. Veal, Jr., *Phys. Rev.* **B10**, 1290 (1974).
- ²¹P. M. Tomchuk, *Ukr. Fiz. Zh.* **24**, 182 (1979).
- ²²W. E. Pickett and P. B. Allen, *Phys. Rev.* **B11**, 3599 (1975).

Translated by Cathy Flick